Computers and Electrical Engineering 38 (2012) 1262–1277

Contents lists available at SciVerse ScienceDirect

Computers and Electrical Engineering

journal homepage: www.elsevier.com/locate/compeleceng

Shock coupled fourth-order diffusion for image enhancement ☆

P. Jidesh *, Santhosh George

Department of Mathematical and Computational Sciences, National Institute of Technology, Karnataka, Srinivasanagar, Mangalore 575 025, India

ARTICLE INFO

Article history:
Available online 23 April 2012

ABSTRACT

In this paper a shock coupled fourth-order diffusion filter is proposed for image enhancement. This filter converges at a faster rate while preserving and enhancing edges, ramps and textures present in the images. The proposed filter diffuses with varying magnitudes in the directions normal to the level-curve and along it. The magnitude of the directional diffusion is controlled by a diffusion function, meant to provide a good response in the direction along the level-curves, than across them. The proposed filter can still preserve the planar approximation of the image, thereby avoiding the discrepancy caused due to the *staircase* effect, as in the second-order counterparts. The anisotropic property of the filter is thoroughly studied, analyzed and demonstrated with perspective and quantitative results. The performance of the proposed filter is compared with the state-of-the-art methods for image enhancement. The quantitative and perspective measures provided endorse the capability of the method to enhance various kinds of images.

1. Introduction

Image reconstruction is an important pre-processing step in majority of the image processing applications. An image reconstruction is to reconstruct the original image $I(x,y)$ from the observed noisy and blurred image $I_0(x,y)$. An image degradation model is generally formulated as:

$$I_0(x,y) = KI(x,y) + \eta(x,y), \tag{1}$$

where $I_0(x,y)$ is the observed blurred and noisy image defined on Ω; $\Omega \subset R^2$ denotes an open bounded set with a Lipschitz boundary, $I(x,y)$ is the original image, $K : X \to Y$ is a linear bounded operator,[1] where X and Y are normed linear spaces and η is a Gaussian white noise with mean zero and variance σ^2. However, the image reconstruction does not belong to a class of well-posed problems in the sense of Hardmard [1], hence some regularization approaches are to be employed to solve them.

There have been a considerable interest in the field of partial differential equations (PDE) and variational methods for image reconstruction in the last few decades [2–10]. Majority of models proposed in the literature include a prior knowledge into the scale space evolution, which leads to an image enhancement, denoising while preserving some of semantically important information like edges, lines etc., present in the images. These methods are widely used in the area of computer vision and image processing. A detailed survey of these methods can be found in [11,12].

Introduction of shock filters by Rudin and Osher can be considered as a peer-less achievement in the area of image enhancement, see [13]. These filters can be classified into a set of hyperbolic PDEs, which create strong discontinuities at

☆ Reviews processed and recommended for publication to Editor-in-Chief by Deputy Editor Dr. Ferat Sahin.

* Corresponding author. Address: Room #MACS 1-2, Department of Mathematical and Computational Sciences, National Institute of Technology, Karnataka, Srinivasanagar, Mangalore 575 025, India. Tel.: +91 824 2474000x3253.

E-mail addresses: jidesh@nitk.ac.in, ppjidesh@gmail.com (P. Jidesh), sgeorge@nitk.ac.in (S. George).

[1] Assuming the shift invariance and linearity of the operator K, it can be modeled as a convolution operation with a blurring kernel $j(x,y) = \frac{1}{4\pi\sigma} e^{-(x^2+y^2)/4\sigma}$, where σ is the standard deviation.

0045-7906/$ - see front matter © 2012 Elsevier Ltd. All rights reserved.
http://dx.doi.org/10.1016/j.compeleceng.2012.03.017

the image edges. However, most of images used commonly are corrupted by noise, in such cases, the shock filter fails to distinguish the inflection points due to the noise from that due to the edges. Many modifications were suggested in subsequent works to address this issue, see [14–16]. In [6,14,17], the authors used a Gaussian smoothed image function in the shock filter, so that the noise gets suppressed to an extend, while the shock is being applied on the edges. However, this method will smooth-out the noise, at the cost of weakening edges. Another mile-stone in this direction was the introduction of "diffusion coupled shock filter" by Alvarez and Mazorra in [14]. Since then, there were many modifications suggested for the diffusion term as well as the shock term, see [6,16–18].

All these filters that couple a diffusion term and a shock term, use a variation of mean curvature motion (MCM) in place of the diffusion term. The MCM was introduced to image processing by Marquiana and Osher in [19]. In the MCM model, each of the level-curves in the image evolves with the speed proportional to their mean curvature and eventually results in making the curved edges more curvy, until it vanishes to a point. In addition to this, all the second-order diffusion methods including MCM approximates the observed image with piece-wise constant images and the evolution eventually results in forming constant patches in the filtered image. This is commonly known as *block* effect or *staircase* effect and it causes visual discrepancies in the filtered image.

In this paper, we propose a fourth-order diffusion coupled shock filter to denoise and deblur the images. By combining the fourth-order diffusion along with the shock term, we can exploit the characteristics inherent in fourth-order diffusion filters to denoise the images, while enhancing the edge features by the shock term. The experimental results are provided for textured and non-textured images and the results of the proposed filter are compared qualitatively and quantitatively, with the most relevant image enhancement methods in the literature.

This paper is organized in five sections. Section 2 gives a mathematical background of the shock filters and explains about some of the relevant shock and diffusion filters proposed in the literature for image restoration. Section 3 highlights the proposed method and its numerical implementation. Section 4 elaborates on the experimental results and their comparison with the existing methods for image enhancement. The last section concludes the work.

2. The background of shock and denoising filters

Though, the second-order non-linear anisotropic diffusion methods can enhance the images when they conditionally evolve towards a negative diffusion, they are highly unstable [7] and hence a unique solution is not guaranteed in such cases [20]. This issue was address by the introduction of a stable hyperbolic PDE called "shock" filter.

A "classical" shock filter was introduced by Rudin and Osher in [13] for image enhancement. The shocks are developed at the inflection points (second derivatives), while the local extrema remains unchanged in each evolution, no new local extrema is introduced as a part of evolution and the steady state solution will have discontinuities at the inflection points. These properties approximate this filter to a deconvolution filter, which can deblur the images.

The idea of shock filter is based on hyperbolic equations theory. For one-dimensional (1D) signals or images, $\phi(I, \nabla I, \nabla^2 I) = \zeta I_x$, where ζ is a constant, I_x denotes the first derivative along the direction x, ∇I and $\nabla^2 I$ denote the gradient and "Laplacian" of the image I, respectively. For any general image processing problem ϕ denotes the function that represents the rate of change of the image function ($\frac{dI}{dt}$). Hence, the solution for the equation $\frac{dI}{dt} = \phi(I, \nabla I, \nabla^2 I)$ under the boundary condition $\frac{\partial I}{\partial \hat{n}} = 0$, where $\hat{n}$ is the unit normal and initial condition $I(x,t) = I_0(x,t)$ is $I(x,t) = I_0(x + at)$, where a is the speed of translation of the solution. The idea behind the shock filter is to make the speed of translation depend on the image structure I_{xx} in case of 1D signals and $I_{\eta\eta}$ in case of two-dimensional (2D) images. Here $\eta = \nabla I/|\nabla I|$ denotes the direction along the gradient ∇I. Now, replacing the speed of translation a with $-sign(I_{\eta\eta})$, for 2D images we obtain the expression of the "classical" shock filter:

$$I_t = -sign(I_{\eta\eta})\|\nabla I\|, \tag{2}$$

where I_t stands for $\frac{\partial I}{\partial t}$, $\|.\|$ denotes the Euclidean norm and *sign* function is defined as:

$$sign(x) = \begin{cases} -1 & \text{if } x < 0 \\ 0 & \text{if } x = 0 \\ +1 & \text{if } x > 0. \end{cases} \tag{3}$$

All the *sign* functions used throughout this paper follows the above definition.

One of the major issues with the "classical" shock filter is, it does not discriminate the noise inflection points from that of the image inflection points (caused by the edges) in a noisy image. Note that, the hyperbolic PDE in (2) obeys the Neumann boundary condition:

$$\frac{\partial I}{\partial \vec{n}} = 0, \tag{4}$$

where $\vec{n}$ is the outward normal to the level curve, and initial condition:

$$I(x, y, 0) = I_0(x, y), \tag{5}$$

where I_0 is the initial image. Throughout this paper we assume the boundary condition (4) and the initial condition (5) for all the PDEs, unless stated otherwise. The hyperbolic PDE in (2) is an anisotropic one, which gives a " shock" in the direction of gradient and does not have any effect in the direction of isophotes (level-curves). The major drawback of the filter in (2) is, along with the edges and finer details the noise features also get enhanced.

2.1. Denoising filters

The second-order non-linear diffusion method proposed by Perona and Malik [7] is a remarkable advancement in the field of PDE based image processing. This non-linear PDE is forward parabolic in general, and inverse or backward parabolic under certain conditions. The PDE denoises the images considering the edges and finer details during the forward process and enhances the image features during the backward process [7]. Though, enhancement is desirable in many scenarios, the enhancement as a consequence of inverse diffusion is highly unstable [20]. The energy functional associated with the PDE is non-convex when the inverse diffusion happens, this non-convex nature of the functional results in a non-unique solution for the associated gradient descent process.

Another prominent issue with the second-order non-linear diffusion methods is that, they approximate the observed image with piece-wise constant images. Therefore, PDE evolution eventually results in forming piece-wise patches during the early stages of evolution and finally these patches combine to form a level image. This level image is the only minimum of the energy functional associated with the second-order PDE. Similarly, during the inverse diffusion any piece-wise constant image is a global minimum of the energy functional, therefore, the blocks will appear in the early stages of evolution and they remain without any change during the course of evolution. This results in the *staircase* effect.

The higher-order PDE's were introduced in the literature to handle the *staircase* effect [5,9]. One of such filters was proposed by You and Kaveh in [9]. In this work the authors proposed a fourth-order diffusion filter that can handle the *staircase* effect considerably. The energy functional proposed in this work is:

$$E(I) = \int_{\Omega} f(\|\nabla^2 I\|)\, dxdy. \tag{6}$$

Here $f(.)$ is an increasing function of the smoothness of the image measured by $\nabla^2 I$ (*Laplacian* of the image). So, the minimization of the energy functional is equivalent to the smoothing of the image. Note that, the *Laplacian* of the pixels will be zero in the planar neighborhood. Therefore, this PDE tries to remove the noise while preserving the edges by approximating the observed image with a piece-wise planar image, which is the only minimum of the energy functional described in (6). The planar approximation eventually results in a reduced *staircase* effect and a more natural outlook to the filtered output. The evolution equation can be straight away formulated as:

$$\frac{\partial I}{\partial t} = -\nabla^2\left(c\left(\|\nabla^2 I\|\right)\nabla^2 I\right), \tag{7}$$

where $\|.\|$ is the Euclidean norm. The diffusion coefficient $c(.)$ is a non-increasing function of the absolute *Laplacian* of the image function, defined as:

$$c(\|\nabla^2 I\|) = \frac{k^2}{k^2 + \left(\|\nabla^2 I\|\right)^2}, \tag{8}$$

here k is the contrast parameter.

Even-though, the fourth-order PDE equation in (7) is capable of removing the noise by penalizing less on the edges and without causing any *staircase* effect, the convergence rate is very slow for this PDE. Besides, the ramp edges are not well preserved in the evolution process, see [21] for details. These two issues of (7) were addressed by Hajiaboli in [21]. In [21], the author replaces the *Laplacian* of the image in the diffusion coefficient function with the gradient magnitude of the image. The diffusion equation considered in [21] is:

$$\frac{\partial I}{\partial t} = -\nabla^2\left(c(\|\nabla I\|)\nabla^2 I\right), \tag{9}$$

where $c(.)$ is a non-increasing function bounded in $(0,1]$. Here $c(.)$ is defined as:

$$c(\|\nabla I\|) = \frac{1}{1 + (\|\nabla I\|/k)^2}. \tag{10}$$

The filter in (9) can still support the planar approximation of the image and avoid the *staircase* effect. The *ramp* preservation capacity of the filter can be explained by considering the fact that: $\frac{\partial I}{\partial t} \to 0$ as $\nabla I \to 0$.

The filter given in (9) can also address the slow convergence rate of (7) and preserve the ramp edges. However, the isotropic nature of this filter makes it a second choice, when it comes to the denoising of images with edges and textures. The edge descriptor ($\nabla^2 I$) in this case is the *Laplacian* operator, which is isotropic in nature and diffuses in all directions equally. Another improved filter was proposed in the literature by Hajiaboli in [22], which is a fourth-order generalization of a second-order filter proposed by Carmona and Zhong in [23]. The filter proposed in [22], uses directional derivatives for

smoothing the images in place of the *Laplacian* operator. This results in different diffusion magnitudes in different directions such that, the speed of diffusion is more along the edges than across them. The aforementioned property makes it an anisotropic filter, which can remove the noise effectively in all the regions including the edges, penalizing less on the edge features. This modified filter can be formulated as:

$$\frac{\partial I}{\partial t} = -\nabla^2 c_1 (c_2 I_{\eta\eta} + c_3 I_{\xi\xi}), \tag{11}$$

where c_1, c_2 and c_3 are the diffusivity functions which control the amount of diffusion in different directions. Here η represents the direction along the gradient, ξ the direction along the isophotes and $I_{\xi\xi}$ denotes the MCM and is defined as:

$$I_{\xi\xi} = -\|\nabla I\| div\left(\frac{\nabla I}{\|\nabla I\|}\right), \tag{12}$$

see [19] for details. The diffusivity functions can be appropriately tuned to get different magnitudes of diffusion in different directions. In [22], the author has chosen $c_1 = c_2 = c(\|\nabla I\|)$ and $c_3 = 1$. With these substitutions, (11) can be rewritten as:

$$\frac{\partial I}{\partial t} = -\nabla^2 \left(c(\|\nabla I\|)^2 I_{\eta\eta} + c(\|\nabla I\|) I_{\xi\xi}\right), \tag{13}$$

where $c(.)$ is a non-increasing function as in (10) and $c(\|\nabla I\|) = 1$ when $\|\nabla I\| = 0$ (in the homogeneous areas). Under this condition, the diffusion equation can be modified as:

$$\frac{\partial I}{\partial t} = -\nabla^2 (I_{\eta\eta} + I_{\xi\xi}). \tag{14}$$

From the above equation, one can find that the filter in (13) acts like an isotopic filter in the smooth (homogeneous) areas, where $\|\nabla I\| = 0$. When $c(\|\nabla I\|) \neq 1$ the filter acts like an anisotropic filter with varying diffusion magnitudes in different directions. Furthermore, it can be easily observed that $c(\|\nabla I\|)^2 \leqslant c(\|\nabla I\|)$ because $c(\|\nabla I\|) \leqslant 1$, hence, the extent of diffusion will be more in the direction of isophotes as compared to the direction of the gradient.

2.2. Shock coupled diffusion

The denoising alone may not be sufficient for many practical applications where the images are of low contrast, the edges are not prominently visible or even the imaging system artifacts can cause the images to be blurry. All these facts motivate one to seek for a method to enhance the images while denoising them. This is the reason for opting a shock filter coupled with diffusion.

Many improvements were suggested for "classical" shock filter in (2), see [14,15,17]. One of such modifications was suggested by Alvarez et al. in [14]. They proposed to use a curvature based diffusion along with the shock term to suppress the noise enhancing property of the "classical" shock filter in (2). This filter is formulated as:

$$I_t = -sign(G_\sigma * I_{\eta\eta})\|\nabla I\| + \lambda I_{\xi\xi}, \tag{15}$$

here λ denotes the control parameter, which is a positive scalar value that controls the magnitude of diffusion, $G_\sigma * I$ denotes the Gaussian (with standard deviation σ) convolved version of the image I, η is the direction along the gradient and ξ is the direction perpendicular to the gradient. This anisotropic filter will act like, a "shock" filter in the direction of gradient and a diffusion filter in the direction perpendicular to the gradient. The term $I_{\xi\xi}$ denotes MCM as defined in (12), where each of the level curves in the image moves in the normal direction at a speed proportional to their mean curvature. In fact, all the second-order anisotropic diffusion methods evolve towards formation of a level-image (which is the only minimum associated with the energy functional) causing the *staircase* effect.

3. Proposed method

All the facts discussed above motivated us to use a fourth-order diffusion term in (13) along with the shock term to enhance images. This shock coupled diffusion filter can denoise the images anisotropically, while preserving the edges (including ramp edges), without causing any *staircase* effect and will converge at a faster rate. Hence, we propose to fit the fourth-order diffusion term in (13) along with a modified version of the shock term proposed in [14]. The proposed filter can be modeled as:

$$I_t = -\frac{2}{\pi} arctan\,(G_\sigma * I_{\eta\eta} \times p(t))\|\nabla I\| - \lambda\nabla^2 \left(c(\|\nabla I\|)^2 I_{\eta\eta} + c(\|\nabla I\|) I_{\xi\xi}\right), \tag{16}$$

where $G_\sigma * I_{\eta\eta}$ is the Gaussian convolved (with the spread of the Gaussian kernel σ) version of $I_{\eta\eta}$ and $p : \mathbb{R}^+ \to (0, 1]$, ($\mathbb{R}$ is the real space) is a non-decreasing function of time defined as:

$$p(t) = \begin{cases} n \times \Delta t & \text{if } n \times \Delta t < 0.5 \\ 1 & \text{otherwise,} \end{cases}$$

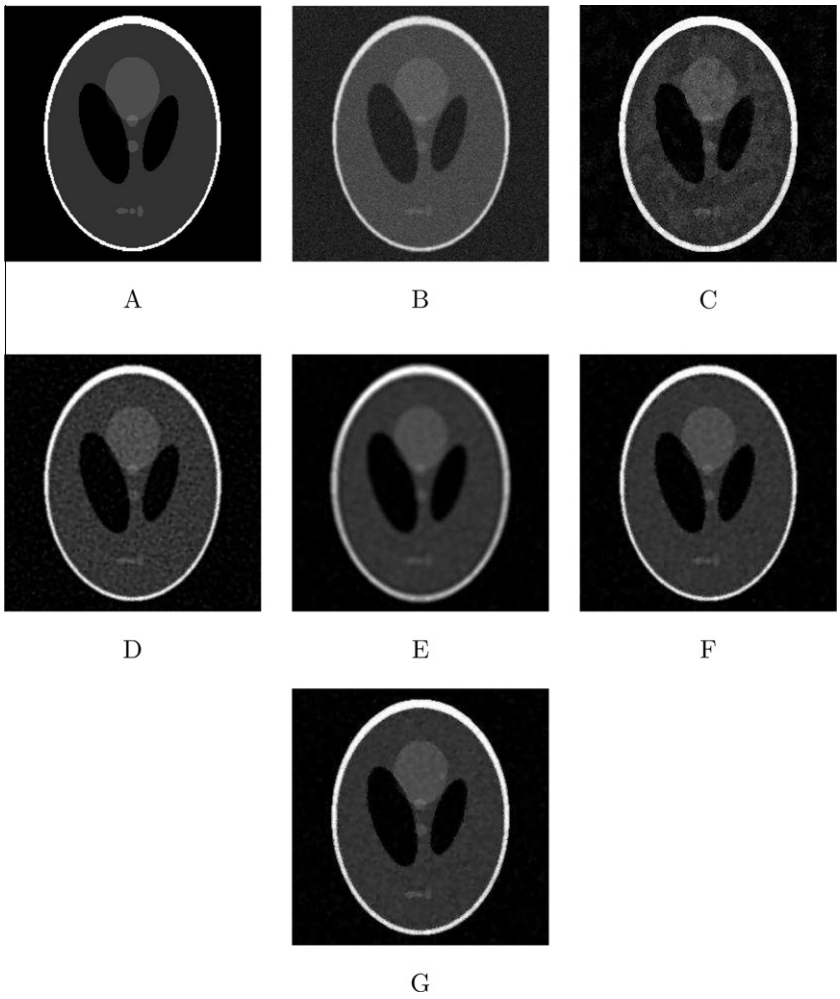

Fig. 1. Image "Phantom": (A) Original figure. (B) Blur and noisy image (out of focus blur: SNR 8 dB). (C) After applying second-order shock proposed by Alveraz et al. [14]. (D) After applying fourth-order method proposed by You and Kaveh [9]. (E) After applying fourth-order method proposed by Tai et al. [5]. (F) After applying method by Hajiaboli [22]. (G) After applying the proposed method.

where $n = 1, 2, 3 \ldots$ is the iteration number and Δt is the time step. The *arctan* function is a "soft *sign* function", which provides a more natural outlook to the enhanced image [16], therefore, we use this function instead of the *sign* function in (15). The *sign* function (3) is a discontinuous function whereas the *arctan* function is a continuously varying function in the open interval $(-\pi/2, +\pi/2)$ for the real input values. Therefore, the *arctan* function behaves smoothly for the input quantity $G_\sigma * I_{\eta\eta} \times p(t)$, which is real. As one can notice, the filter in (16) has two terms a shock term (the first term), which provides a shock at the inflection points (second derivatives) and a diffusion term (the second term), which suppresses the noise features. The parameter λ is a positive scalar value, which controls the magnitude of shock and diffusion. The function $c(.)$ is a non-increasing function as defined in (10). The terms $I_{\eta\eta}$ and $I_{\xi\xi}$ are the second-order directional derivatives along the gradient and the isophotes, respectively. The other notations are as in (15). The function $p(t)$ inside the *arctan* function controls the effect of shock during the early stages of evolution, because during the initial phases of evolution the noise will be dominating the image, hence, the effect of shock filter only helps to enhance the noise features. Incorporating a function of time with the shock term can reduces the effect of shock during the initial stages of evolution. The function $p(.)$ returns small values much less than 1 during the initial stages of evolution (iteration), making magnitude of the shock very less, therefore, the filter acts like a normal anisotropic diffusion filter. After a finite number of iterations the function $p(.)$ always returns '1'. Thereafter, the filter acts like a shock coupled diffusion filter regularized by the control parameter λ.

3.1. Numerical implementation

We use the explicit Euler numerical schemes for solving the PDEs given in (16). Since the *shock* filters are hyperbolic PDEs, the usual central difference schemes may not help in getting proper results. This scheme will be highly unstable and may not

Fig. 2. Image "Lena": (A) Original figure. (B) Blur and noisy image (out of focus blur: SNR 8 dB). (C) After applying second-order shock proposed by Alveraz et al. [14]. (D) After applying fourth-order method proposed by You and Kaveh [9]. (E) After applying fourth-order method proposed by Tai et al. [5]. (F) After applying method by Hajiaboli [22]. (G) After applying the proposed method.

converge. So we use the *upwind* scheme proposed in [24]. The scale space parameter h is assumed to be 1 and Δt is the time step. Using the *upwind* for solving $\|\nabla I\|$ in the shock term of (16) will result in the following expressions.

$$\|\nabla I\| = \sqrt{D_x^2 + D_y^2}, \tag{17}$$

where $D_x = minmod(I_x^+(x,y), I_x^-(x,y))$, $D_y = minmod(I_y^+(x,y), I_y^-(x,y))$ the *minmod* operator is defined as:

$$minmod(x,y) = \begin{cases} min(|x|,|y|) & \text{if } xy > 0 \\ 0 & \text{otherwise,} \end{cases}$$

where

$$\begin{aligned} &I_x^+(x,y) = I(x+1,y) - I(x,y), \\ &I_x^-(x,y) = I(x,y) - I(x-1,y), \\ &I_x(x,y) = (I_x^+ + I_x^-)/2, \\ &I_y^+(x,y) = I(x,y+1) - I(x,y), \\ &I_y^-(x,y) = I(x,y) - I(x,y-1) \\ &\text{and } I_y(x,y) = (I_y^+ + I_y^-)/2. \end{aligned}$$

The explicit Euler equation with finite central difference scheme is used for the rest of the terms in differential Eq. (16):

Fig. 3. Image "Woman": (A) Original figure. (B) Blur and noisy image (out of focus blur: SNR 8 dB). (C) After applying second-order shock proposed by Alveraz et al. [14]. (D) After applying fourth-order method proposed by You and Kaveh [9]. (E) After applying fourth-order method proposed by Tai et al. [5]. (F) After applying method by Hajiaboli [22]. (G) After applying the proposed method.

$$I_{\eta\eta} = \frac{I_{xx}|I_x|^2 + 2I_{xy}I_xI_y + I_{yy}|I_y|^2}{1 + |I_x|^2 + |I_y|^2}, \tag{18}$$

$$I_{\xi\xi} = \frac{I_{xx}|I_y|^2 - 2I_{xy}I_xI_y + I_{yy}|I_x|^2}{1 + |I_x|^2 + |I_y|^2}, \tag{19}$$

$$\begin{aligned} I_{xx} &= I(x+1,y) - 2I(x,y) + I(x-1,y),\\ I_{yy} &= I(x,y+1) - 2I(x,y) + I(x,y-1),\\ I_{xy} &= (I_x(x+1,y) - I_x(x,y-1))/2. \end{aligned} \tag{20}$$

Let

$$g(\|\nabla I\|) = c(\|\nabla I\|)^2 I_{\eta\eta} + c(\|\nabla I\|) I_{\xi\xi}. \tag{21}$$

Then

$$\nabla^2 g^n_{x,y} = g^n_{x+1,y} + g^n_{x-1,y} + g^n_{x,y+1} + g^n_{x,y-1} - 4g^n_{x,y}. \tag{22}$$

With the help of above discretization equations one can write the full discretization for the filter in (16).

4. Experimental results and discussions

We used a synthetic image "Phantom" (a constant intensity image), a natural image "Lena" (a partially textured image) and two partially textured natural images "Woman" and "Boat" to test the performance of our algorithm. In all the

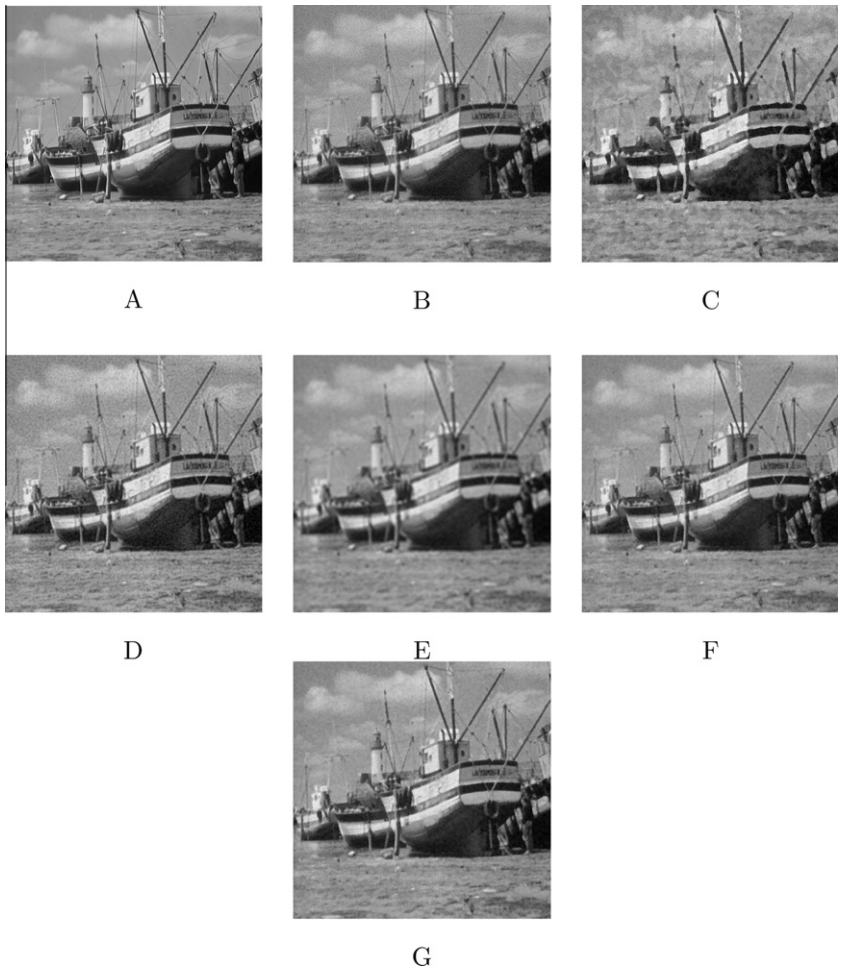

Fig. 4. Image "Boat": (A) Original figure. (B) Blur and noisy image (out of focus blur: SNR 8 dB). (C) After applying second-order shock proposed by Alveraz et al. [14]. (D) After applying fourth-order method proposed by You and Kaveh [9]. (E) After applying fourth-order method proposed by Tai et al. [5]. (F) After applying method by Hajiaboli [22]. (G) After applying the proposed method.

experiments the intensity values of the images are normalized to the range [0–1]. Though, the quality of the filtered output can be visually compared, we provide quantitative measurements for the performance of various methods cited in this work along with the proposed one. We use three different image quality metrics signal-to-noise ratio (SNR), Pratt's figure of merit (P-FOM) [25] and structural similarity index metric (SSIM) [26] to compare the performance of our method to the other relevant methods in the literature.

4.1. Image quality measures

The SNR [27] is a commonly used measure to quantify the denoising capability of a filter. The SNR is defined as:

$$\mathrm{SNR} = 10\log_{10}\left(\sigma_f^2/\sigma_n^2\right), \tag{23}$$

where $\sigma_f^2$is the variance of the noise free image and σ_n^2 is the variance of the noise. A larger SNR value indicates a better image-denoising capacity.

The efficiency of any enhancement method is measured in terms of its capability to retain the edges while removing the noise. The edge preservation capability of various enhancement methods are compared using Pratt's figure of merit (P-FOM) [25] defined as:

$$\mathrm{FOM} = \frac{1}{max\{\widehat{N}, N_{ideal}\}} \sum_{i=1}^{\widehat{N}} \frac{1}{1 + d_i^2 \alpha}, \tag{24}$$

where $\widehat{N}$ and N_{ideal} are the number of detected and ideal edge pixels, respectively, d_i is the Euclidean distance between the ith detected edge pixel and the nearest ideal edge pixel, and α is a constant typically set to 1/9. FOM ranges between 0 and 1,

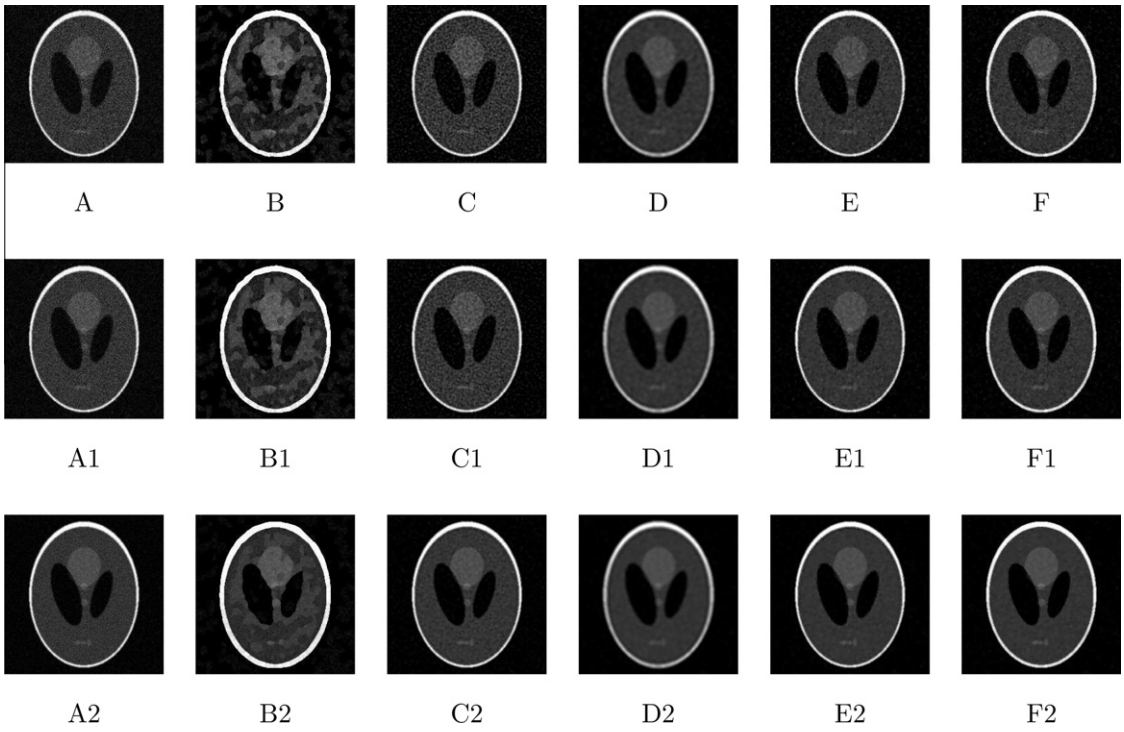

Fig. 5. Filtered results at different noise levels: (A), (A1) and (A2). The blur-noisy image with SNR 6, 7 and 9 dB, respectively (B), (B1) and (B2). After applying second-order shock proposed by Alveraz et al. [14] (C), (C1) and (C2). After applying fourth-order method proposed by You and Kaveh [9] (D), (D1) and (D2). After applying fourth-order method proposed by Tai et al. [5] (E), (E1) and (E2). After applying method by Hajiaboli [22] (F), (F1) and F(2). After applying the proposed method.

with unity for ideal edge detection. We apply the Canny edge detector [28] for locating the edges. The standard deviation of the Gaussian kernel in the Canny detector is chosen as $\sigma = 0.1$.

In addition to the above two measures, the structure similarity (SSIM) index is used to compare the luminance, contrast and structure of two different images [26]. SSIM is formulated as:

$$\mathrm{SSIM}(x,y) = \frac{(2\mu_x\mu_y + C1) \times (2\sigma_{xy} + C2)}{(\mu_x^2 + \mu_y^2 + C1)(\sigma_x^2 + \sigma_y^2 + C2)}, \tag{25}$$

where x and y denotes the content of local windows in original and reconstructed images, respectively, σ_{xy} is the covariance of x and y, σ_x^2 and σ_y^2 denotes the variance of x and y, respectively and $C_1 = (k_1 L)^2, C_2 = (k_2 L)^2$, where L is the dynamic range of pixels values, $k_1 = 0.01$ and $k_2 = 0.03$ are constants. The measure is applied for non-overlapping windows in both the images (original and reconstructed). In this work we measure mean-SSIM (MSSIM) which is an index to evaluate the overall image quality. It is defined as:

$$\mathrm{MSSIM}(X,Y) = \frac{1}{M}\sum_{j=1}^{M}\mathrm{SSIM}(x_j, y_j), \tag{26}$$

where X and Y are the original and reconstructed images, respectively; x_j and y_j denotes the content of the jth local window in reference and distorted images, respectively and M is the number of local windows in the image.

4.2. Experimental set-up

The test images are corrupted by Gaussian noise making the SNR of the noisy image 8 dB (decibel) and we have chosen a value 5 for the standard deviation σ in the Gaussian smoothing function G in the expression (16). A blurred image (out-of-focus blur) is generated using a Gaussian smoothing function with standard deviation $\sigma = 4$. The scale space parameter $h = 1$. The time step $\Delta t = 0.01$ for all the fourth-order methods except the fourth-order regularization method in [5]. For this method the time step is chosen as $\Delta t = 0.002$, because the method is highly sensitive to the time step.

In each experiment, the performance of the proposed method was compared to that of other filters like: forth-order denoising by You and Kaveh [9], regularized fourth-order denoising technique by Tai et al. [5], the modified fourth-order method proposed by Hajiaboli in [21,22] and the shock filter proposed by Alvarez et al. in [14]. The performance of each method is

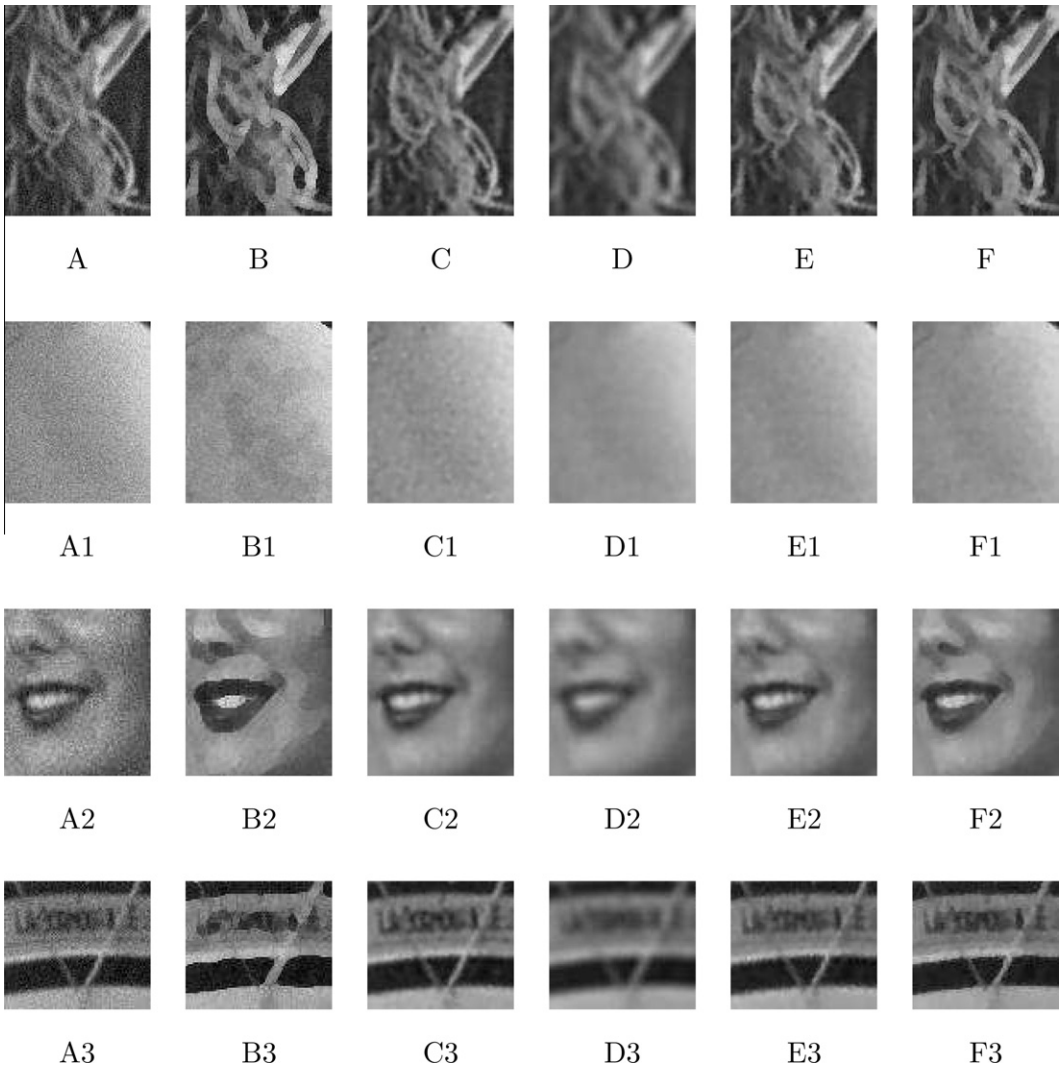

Fig. 6. The enlarged portions of the images "Lena", "Woman" and "Boat", filtered with different methods: A, A1, A2 and A3. Noisy image, B, B1, B2 and B3. Alvarez model C, C1, C2 and C3. You–Kaveh method D, D1, D2 and D3. Tai's method E, E1, E2 and E3. Hajiaboli method F, F1, F2 and F3. The proposed method.

quantified in terms of different quality measures defined above. The performance of each method is demonstrated and compared in the subsequent sections.

4.3. Results and analysis

The visual results of applying different enhancement techniques on the image: "Phantom" are shown in Fig. 1C–G. This image is a non-textured image with constant intensity regions. The "Phantom" image consists of regions with different contrast and geometric shapes. We choose the value 0.06 for the parameter λ in our experiments. The blurred and noisy image (shown in Fig. 1B) is used as an input to different image enhancement methods in the literature along with the one proposed in this paper. The output results shown are quite in favor of the claim that, the proposed method enhances the edges and denoises the images better than the other methods shown in the results.

The results of different methods in the literature along with the proposed method when applied to a partially textured natural image "Lena" is shown in Fig. 2C–G. The results of various methods including the proposed method applied on the natural images "Woman" and "Boat" are shown in Figs. 3 and 4, respectively. One can visualize from the figures; Figs. 1–4 that the proposed method performs better (in terms of enhancement) than the other methods.

The experiments are conducted for various noise levels. Fig. 5 shows the perspective results of various filters applied to the image "Phantom" corrupted by three different noise-levels. The filtered results are shown for the input noise level 6, 7

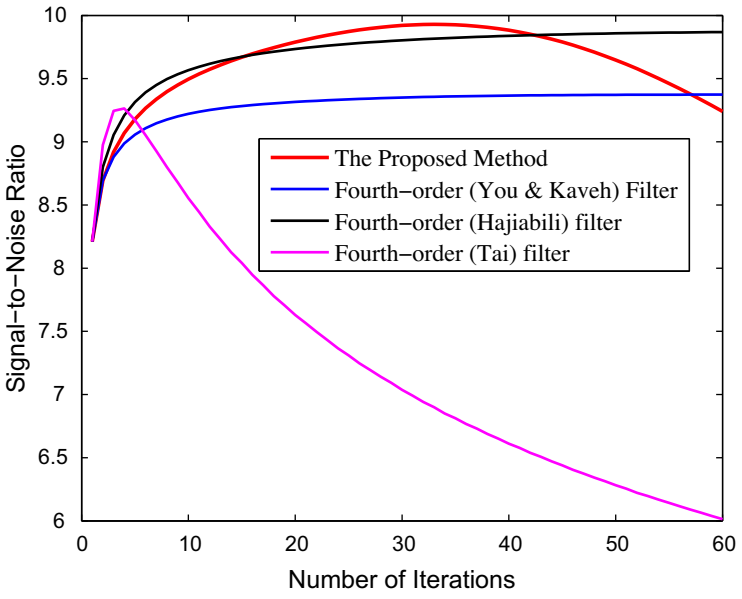

Fig. 7. The signal-to-noise ration (SNR) plotted in each iterations for the image "Phantom": SNR of the initial noisy image 8 dB.

Table 1
The optimal number of iterations for different methods for various noise levels (SNR in dB) for the image: "Phantom".

Methods	SNR = 6 dB	SNR = 7 dB	SNR = 8 dB	SNR = 9 dB	SNR = 10 dB
You–Kaveh	150	140	135	130	126
Tai et al.	11	9	8	7	5
Hajiaboli	120	111	104	96	90
Proposed method	61	52	43	36	31

and 9 dB (SNR), respectively. The noisy image is shown in the first column of Fig. 5 and consecutive columns show the results of various methods in the literature. The last column [(F), (F1) and (F2)] shows the result of the proposed method. The proposed filter performs better compared to the other methods, in all the different input noise levels.

Fig. 6 shows enlarged portions (textured and homogeneous regions) of the image "Lena", "Woman" and "Boat" after applying various enhancement methods. Two portions from the image "Lena" and one portion each from image "Woman" and "Boat" are enlarged for a better visibility. The first row shows a highly textured region taken from the image "Lena" and the second one shows a smooth gray level portion from the same image. The third and fourth rows display smooth and partially textured portions of images "Woman" and "Boat", respectively. The first column in Fig. 6, shows the portions of the distorted input image and subsequent columns show the image (portions) after applying various filtering methods. The second column in this figure is the results of applying Alvarez model [14]. In this particular output image; shown in the second column of Fig. 6, one can notice that even though the edges are enhanced the noise features are still present in the filtered output. The reason is; in Alvarez model the shock component will be active right from the initial stages of the filtering process and this will result in enhancing the noise components along with the edges. The third to fifth columns in Fig. 6 are the results of the methods You–Kaveh [9], TAI [5] and Hajiaboli [22], respectively. In all these results one fact is evident: the images are denoised at the cost of weakening the edges. In the proposed method (the output is shown in the last column of Fig. 6) the noise features are considerably removed, because the time dependent function inside the shock term suppresses the effect of shock in the earlier stages of evolution; consequently the noise features gets only diffused during the early stages of evolution process. The edges are enhanced well and noise features are removed considerably in the proposed method.

Table 2
The optimal number of iterations for different methods for various noise levels (SNR in dB) for the image: "Lena".

Methods	SNR = 6 dB	SNR = 7 dB	SNR = 8 dB	SNR = 9 dB	SNR = 10 dB
You–Kaveh	250	235	208	200	190
Tai et al.	22	14	10	8	6
Hajiaboli	220	205	190	178	170
Proposed method	120	110	102	89	80

Table 3
The optimal number of iterations for different methods for various noise levels (SNR in dB) for the image: "Woman".

Methods	SNR = 6 dB	SNR = 7 dB	SNR = 8 dB	SNR = 9 dB	SNR = 10 dB
You–Kaveh	230	225	200	190	178
Tai et al.	19	12	12	9	9
Hajiaboli	210	200	191	180	168
Proposed method	109	100	92	81	70

Table 4
The optimal number of iterations for different methods for various noise levels (SNR in dB) for the image: "Boat".

Methods	SNR = 6 dB	SNR = 7 dB	SNR = 8 dB	SNR = 9 dB	SNR = 10 dB
You–Kaveh	240	235	220	201	188
Tai et al.	24	17	16	12	10
Hajiaboli	221	202	185	176	168
Proposed method	119	107	96	88	79

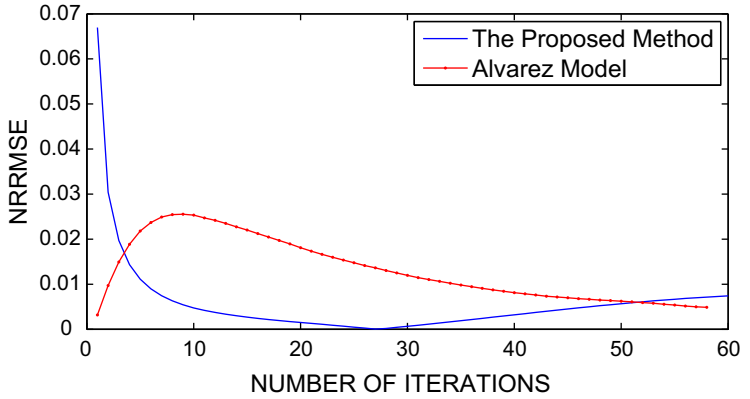

Fig. 8. Normalized root mean square error plotted against the number of iterations for various methods including the proposed one for the image "Phantom" (SNR of the noisy image is 10 dB).

The optimal number of iterations n^2 for each method at a given noise level (here we have chosen the SNR of initial noisy image as 8 dB) is decided based on the SNR values. The iteration number corresponding to the optimal SNR value is taken as the optimal iteration number. The graph in Fig. 7 shows a plot of SNR against the number of iterations for the image "Phantom", the change in SNR with the number of iterations follow the same characteristics for other input images as well. Hence, we only tabulate the optimal number of iterations corresponding to each SNR value for different input images. The optimal iteration numbers obtained based on the SNR values are shown in Tables 1–4, for the input test images "Phantom", "Lena", "Woman" and "Boat", respectively. All the images shown in Figs. 1–4 are taken after the corresponding optimal number of iterations.

The normalized relative root mean square error (NRRMSE) is a measure to indicate the root mean square error in each iteration for a particular method. The NRRMSE keeps on decreasing in each iteration during the diffusion process as the filtered image approaches the original one. NRRMSE is defines as:

$$\mathrm{NRRMSE} = |\mathrm{RMSE}_i - \mathrm{RMSE}_{i+1}|/\mathrm{RMSE}_{i+1}, \tag{27}$$

where RMSE_i denotes the root mean square error in the ith iteration. RMSE for a $M \times N$ image is defined as:

$$\mathrm{RMSE}_i = \left(\frac{1}{N \times M} \sum_{i=1}^{N} \sum_{j=1}^{M} (I_o^i(i,j) - I(i,j))^2 \right)^{1/2}, \tag{28}$$

where I_o^i is the observed image at ith iteration and I is the actual image. When the noise gets smoothed out the reconstructed image gets closer to the original one. From Fig. 8 one can observe that, the NRRMSE corresponding to the proposed method is decreasing initially and then it is increasing after some iterations, whereas, for Alvarez model NRRMSE first increases and then it decreases, this effect is due to the shock component present in the filter. In the proposed method the shock will not have significant contribution during the initial stages of evolution therefore, only diffusion will happen, this causes

[2] The iteration number chosen to get optimal performance.

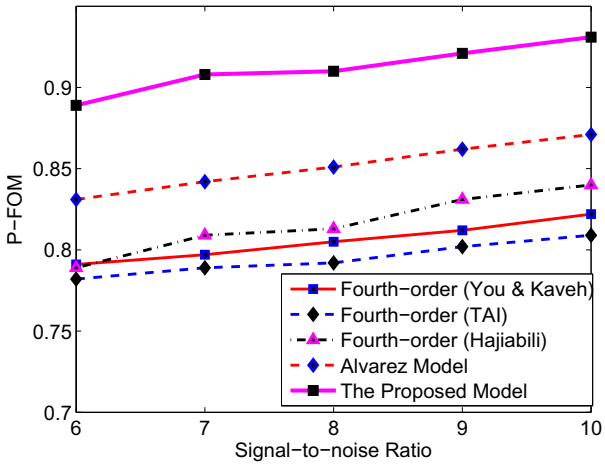

Fig. 9. Pratt's figure of merit (P-FOM) plotted for various methods at different SNR values (in dB) of the input: noisy image (image: "Phantom").

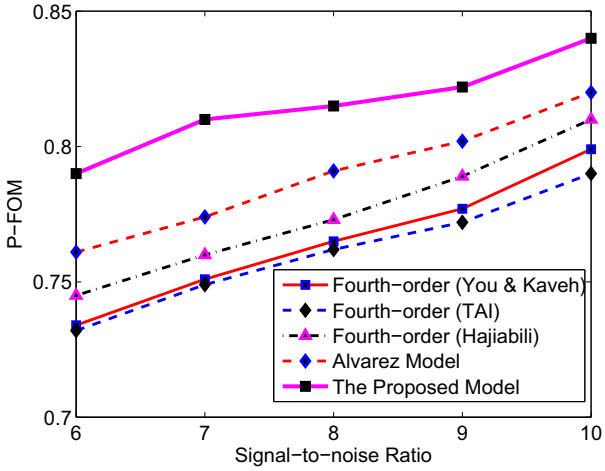

Fig. 10. Pratt's figure of merit (P-FOM) plotted for various methods at different SNR values (in dB) of the input: noisy image (image: "Lena").

the NRRMSE to decrease considerably during the initial stages of evolution whereas, in Alvarez model the shock will be dominant even during the initial stages of evolution. This causes the NRRMSE to increase for first few iterations and then decrease, thereafter.

The Pratt's figure of merit (P-FOM) for the images "Phantom" and "Lena" filtered using different filters (including the proposed one), for various SNR values of the input noisy image are plotted in the graph given in Figs. 9 and 10, respectively. The number of iterations for each method (at various SNR values) for the images "Phantom" and "Lena" are selected based on Tables 1 and 2, respectively. From these graphs one can observe that the edge preserving capacity of the proposed method is better compared to the other methods. The results of applying the Canny edge detector (with $\sigma = 0.1$) on images filtered using various method are shown in Fig. 11. Fig. 11A shows the result of edge detection method applied on the original image. Fig. 11B shows the result for blurred and noisy image. Fig. 11C–F shows the results of the edge detection method applied on the filtered outputs of various methods. The edges detected for the image filtered using the proposed method (shown in Fig. 11G) are more robust than that of the other methods (shown in Fig. 11C–F).

MSSIM measured for the images "Phantom" and "Lena" filtered using different methods (including the proposed one), for various SNR values of the input noisy image are plotted in the graph given in Figs. 12 and 13, respectively. The number of iterations for each method (at various SNR values) are selected based on Tables 1 and 2 for images "Phantom" and "Lena", respectively. From these figures it could be easily verified that the proposed method has good contrast, illumination and the structure preserving capabilities as compared to the other methods.

From all the measures described above we have experimentally (both visually and quantitatively) demonstrated that the proposed method enhances the contrast, texture and edge features present in the image, while removing the noise effectively. The figures shown in favor of the proposed method especially the one that enlarged the constant intensity portion

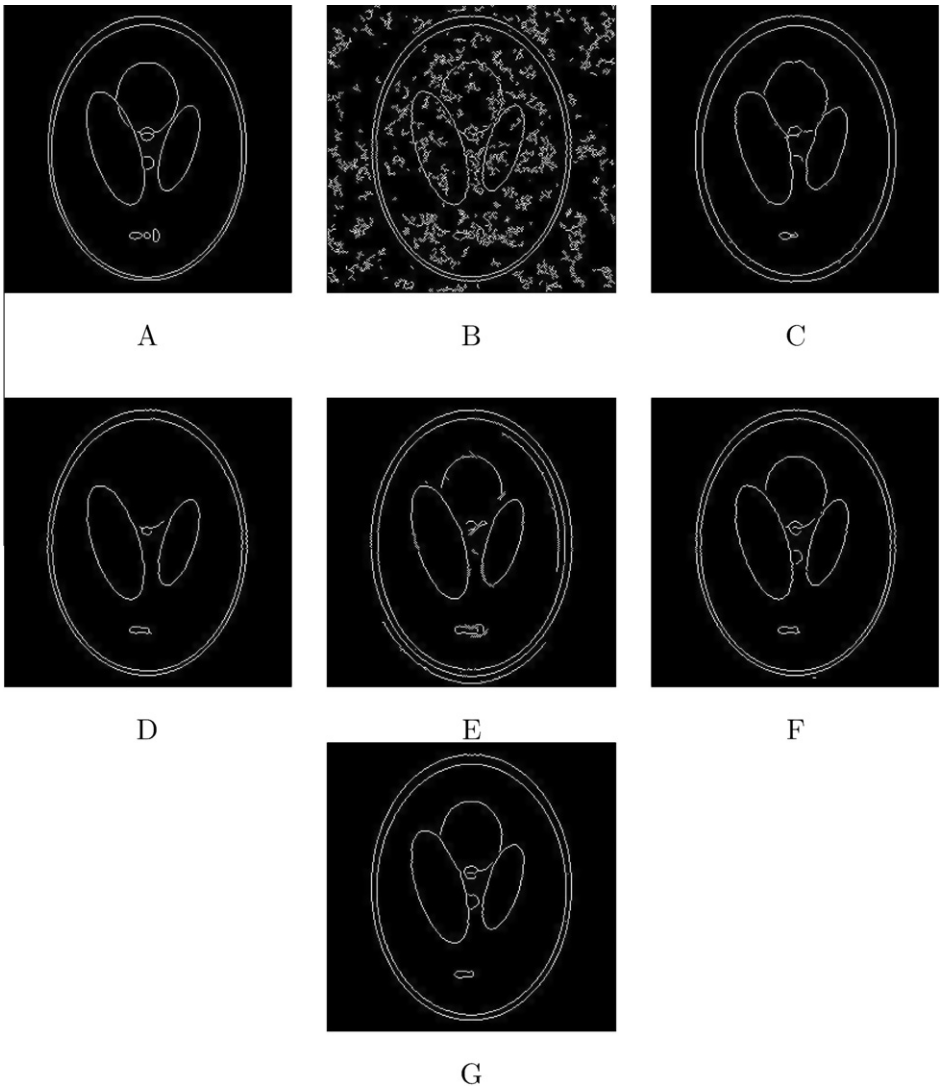

Fig. 11. Result of canny edge detector applied on "Phantom" after filtering with various methods. (A) Original figure. (B) Blur and noisy image (out of focus blur: SNR 8 dB). (C) Alveraz model [14]. (D) You and Kaveh method [9]. (E) Tai model [5]. (F) Hajiaboli model [22]. (G) The proposed model.

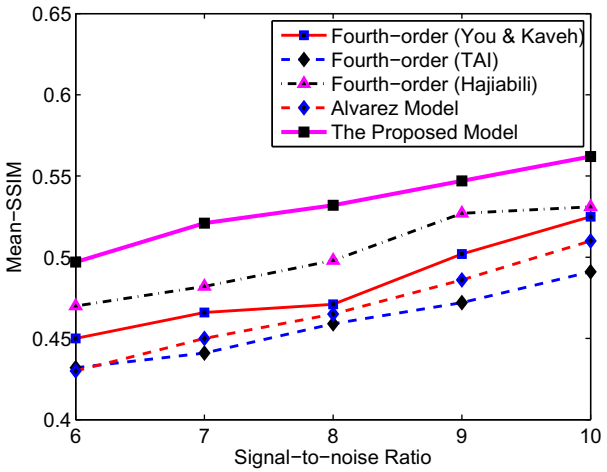

Fig. 12. Mean-structural similarity index (MSSIM) plotted for various methods at different SNR values (in dB) of the input: noisy image (image: "Phantom").

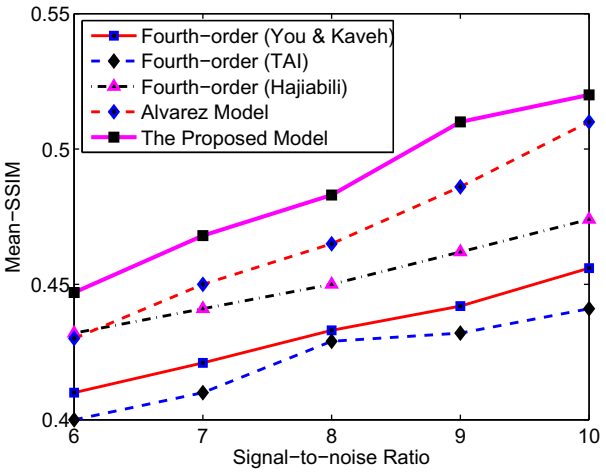

Fig. 13. Mean-structural similarity index (MSSIM) plotted for various methods at different SNR (in dB) values of the input: noisy image (image: "Lena").

gives a clear understanding that the propose method does not contaminate the constant intensity regions with small intensity patches (that causes a visual discrepancy).

Please note that, the quality measures are not provided explicitly for the images "Woman" and "Boat" for the reason that, the measures are similar in characteristic to the image "Lena" (all these images fall into the category of partially textured natural image).

5. Concluding remarks

In this paper we have proposed a fourth-order anisotropic diffusion cum shock filter. The proposed method enhances the semantic features like edges, finer details and textures, while denoising the images as evident from the demonstrated results. The denoising and enhancing capacity of the proposed filter is controlled using a positive scalar regularization parameter. The anisotropic nature of the proposed filter is governed by a diffusion coefficient function, defined using an absolute value of the gradient image. The diffusion coefficient function in our method (driven by the absolute gradient image), has been shown to catalyze the diffusion process. Thus, our method results in a faster process convergence as compared to many other prominent fourth-order methods in the literature. Unlike the second-order methods that use piece-wise constant approximation, our filter adopts a planar approximation, thereby considerably reducing the *staircase* effect. The filtered outputs shown in favor of our proposed method clearly demonstrate the reduced *staircase* effect.

We have introduced a time-dependent function inside the shock term of the proposed filter. This function helps in providing a controlled shock during the initial stages of evolution. We have presented the controlled shock and diffusion aspects of our method with the help of a graph in the result section. Compared to other shock coupled diffusion methods, the proposed method robustly handles the noise and blur at various stages of the evolution process.

The iteration process of our method is controlled using the SNR values in each iteration. The evolution proceeds as long as the SNR increases monotonically and stops at the point when it decreases. Since the iteration process is controlled dynamically in the proposed filter, optimal results are ensured.

We have compared our method with all the relevant image enhancement methods in the literature using the visual results and widely used statistical qualitative measures like SNR, Pratt's FOM and MSSIM. The pictorial and tabulated measures are highly in favor of the proposed method. The proposed method is tested for both textured and non-textured images (including artificial and natural images) at various noise variances. The experimental results provided substantially show the efficiency and effectiveness of the proposed method.

References

[1] Hardmard J. Lecturer on Cauchy's problem in linear partial differential equations, vol. 1. Dover Publication; 1953.
[2] Aubert G, Vese L. A variational method in image recovery. SIAM J Numer Anal 1997;34:1948–79.
[3] Guy G, Sochen NA, Zeevi YY. Image denoising and decomposition with total variation minimization and oscillatory functions. J Math Imaging Vis 2008;20:7–18.
[4] Leonid I, Osher S, Fatemi E. Nonlinear total variation based noise removal algorithms. Physica D 1992;60:259–68.
[5] Lysaker M, Lundervold A, Tai XC. Noise removal using fourth-order partial differential equation with applications to medical magnetic resonance images in space and time. IEEE Trans Image Process 2003;12:1579–90.
[6] Kornprobst P, Deriche R, Aubert G. Image coupling restoration and enhancement via pdeGs. In: Proceedings of the international conference on image processing. IEEE; 1997. p. 458–61.
[7] Perona P, Malik J. Scale-space and edge detection using anisotropic diffusion. IEEE Trans Pattern Anal Mach Intel 1990;12:629–39.
[8] Weickert J. Coherence-enhancing diffusion filtering. Int J Comput Vis 1999;31:111–27.

[9] You YL, Kaveh M. Fourth-order partial differential equations for noise removal. IEEE Trans Image Process 2000;9:1723–30.
[10] Jidesh P, George S. A time-dependent switching anisotropic diffusion model for denoising and deblurring images. J Mod Opt 2012;59:140–56.
[11] Romeny BM. Geometry driven diffusion in computer vision. 2nd ed. Kluwer Academic Publisher; 1994.
[12] Weickert J. A review of nonlinear diffusion filtering. Scale Space Theory Comput Vis 1997;1252:3–28.
[13] Osher S, Rudin LI. Feature-oriented image enhancement using shock filters. SIAM J Numer Anal 1990;27:919–40.
[14] Alvarez L, Mazorra L. Signal and image restoration using shock filters and anisotropic diffusion. SIAM J Numer Anal 1994;31:590–605.
[15] Brockett RW, Maragos P. Evolution equations for continuous scale morphology. In: Proceedings of IEEE international conference on acoustic, speech and signal processing. IEEE; 1992. p. 125–8.
[16] Gilboa G, Sochen NA, Zeevi YY. Regularized shock filters and complex diffusion. In: ECCV 02. Proceedings of the 7th European conference on computer vision – part I. Springer; 2002. p. 399–413.
[17] Coulon O, Arridge SR. Dual echo mr image processing using multi-spectral probabilistic diffusion coupled with shock filters. In: Proceedings of British conference on medical image understanding and analysis. MIUA-London; 2000. p. 458–61.
[18] Weickert J. Coherence-enhancing shock filters. Pattern Recog LNCS 2003;2781:1–8.
[19] Marquiana A, Osher S. Explicit algorithms for a new time-dependent model based on level set motion for nonlinear deblurring and noise removal. SIAM J Sci Comput 2000;22:387–405.
[20] Hollig K. Existence of infinitely many solutions for a forward–backward heat equation. Trans Am Math Soc 1983;278:299–316.
[21] Hajiaboli MR. A self-governing hybrid model for noise removal. In: PSIVT 09. Proceedings of the 3rd Pacific-Rim symposium on advances in image and video technology. Springer; 2009. p. 295–305.
[22] Hajiaboli MR. An anisotropic fourth-order diffusion filter for image noise removal. Int J Comput Vis 2010;20:182–97.
[23] Carmona RA, Zhong S. Adaptive smoothing respecting feature directions. IEEE Trans Image Process 1998;3:353–8.
[24] Osher S, Sethian JA. Fronts propagating with curvature-dependent speed: algorithms based on Hamilton–Jacobi formulation. J Comput Phys 1988;79:12–49.
[25] Pratt WK. Digital image processing. 4th ed. Wiley; 2007.
[26] Wang Z, Bovik AC. Image quality assessment: from error visibility to structural similarity. IEEE Trans Image Process 2004;13:1–14.
[27] Gonzalez RC, Woods RE. Digital image processing. 2nd ed. Upper Saddle River: Prentice Hall; 2001.
[28] Canny J. A computational approach to edge detection. IEEE Trans Pattern Anal Mach Intel 1986;8:679–98.

P. Jidesh received his MCA from National Institute of Technology, Calicut, India and M.Tech. in Computer Science from University of Kerala, India. He is currently working as an Assistant Professor in the Department of Mathematical and Computational Sciences, National Institute of Technology Karnataka (NITK), India. He has guided many M.Tech. dissertations and MCA projects. He has published papers in international journals and proceedings of international conferences in the area of image and signal restoration and enhancement. His research interests include PDE and variational methods in image processing.

Santhosh George received his Ph.D. in Mathematics from Goa University. He is currently working as an Associate Professor in the Department of Mathematical and Computational Sciences, National Institute of Technology Karnataka, India. He has published several papers in international journals of good repute and proceedings of the international conferences. His research interests include functional analysis, inverse and ill-posed problems and its applications. He has supervised many M.Tech. dissertations. Two students were awarded Ph.D. degree under his supervision. Currently three Ph.D. scholars are working under his supervision.